Journal of Neuroscience Research 94:1531–1545 (2016)

Astrocyte-Produced Leukemia Inhibitory Factor Expands the Neural Stem/Progenitor Pool Following Perinatal Hypoxia–Ischemia

Ryan J. Felling,[1,2] Matthew V. Covey,[2] Paul Wolujewicz,[3] Mona Batish,[3] and Steven W. Levison[2]*

[1]Departments of Neurology and Pediatrics, Johns Hopkins University School of Medicine, Baltimore, Maryland
[2]Department of Pharmacology, Physiology and Neuroscience, RBHS–New Jersey Medical School, Newark, New Jersey
[3]Department of Microbiology, Biochemistry and Molecular Genetics, RBHS–New Jersey Medical School, Newark, New Jersey

Brain injuries, such as cerebral hypoxia–ischemia (H-I), induce a regenerative response from the neural stem/progenitors (NSPs) of the subventricular zone (SVZ); however, the mechanisms that regulate this expansion have not yet been fully elucidated. The Notch- Delta-Serrate-Lag2 (DSL) signaling pathway is considered essential for the maintenance of neural stem cells, but it is not known if it is necessary for the expansion of the NSPs subsequent to perinatal H-I injury. Therefore, the aim of this study was to investigate whether this pathway contributes to NSP expansion in the SVZ after H-I and, if so, to establish whether this pathway is directly induced by H-I or regulated by paracrine factors. Here we report that Notch1 receptor induction and one of its ligands, Delta-like 1, precedes NSP expansion after perinatal H-I in P6 rat pups and that this increase occurs specifically in the most medial cell layers of the SVZ where the stem cells reside. Pharmacologically inhibiting Notch signaling in vivo diminished NSP expansion. With an in vitro model of H-I, Notch1 was not induced directly by hypoxia, but was stimulated by soluble factors, specifically leukemia inhibitory factor, produced by astrocytes within the SVZ. These data confirm the importance both of the Notch-DSL signaling pathway in the expansion of NSPs after H-I and in the role of the support cells in their niche. They further support the body of evidence that indicates that leukemia inhibitory factor is a key injury-induced cytokine that is stimulating the regenerative response of the NSPs.

Key words: Notch; subventricular zone; stem cells; astrocytes; stroke; leukemia inhibitory factor; rats

INTRODUCTION

Throughout development, intricately coordinated series of events direct the differentiation of a common set of precursors into a multitude of specific cell types. Even after development has ceased, discrete populations of undifferentiated precursors persist in many tissues including the nervous system. These precursors provide a reserve for both physiologic cell turnover as well as replacement of lost cells due to pathologic processes. Many of the same molecular mechanisms underlying cell fate decisions that occur during development also guide the

SIGNIFICANCE

Studies have shown that the numbers of resident neural stem cells and progenitors in the subventricular zone increase after injury and that these cells can generate new neurons, astrocytes, and oligodendrocytes. However, the extent of cell replacement that normally occurs is modest. The studies reported here reveal the cellular and molecular signals that underlie this regenerative program. On the basis of these findings, new therapeutics can be designed to increase the naturally occurring amplification of the brain's stem cells and progenitors towards enhancing central nervous system regeneration and recovery of neurological function after injury.

This work was supported by grants from the National Institutes of Health (MH59950 and HD052064) and the Leducq Foundation awarded to SWL, NS0469903-01 awarded to RJW, and DP5 OD012160 awarded to MB. The authors have no conflicts of interest to report.

*Correspondence to: Steven W. Levison, PhD, Laboratory for Regenerative Neurobiology, Pharmacology, Physiology and Neuroscience, RBHS–New Jersey Medical School, 205 South Orange Avenue, H-1226, Newark, NJ 07103. E-mail: levisosw@rutgers.edu

Received 29 May 2016; Revised 30 August 2016; Accepted 31 August 2016

Published online 23 September 2016 in Wiley Online Library (wileyonlinelibrary.com). DOI: 10.1002/jnr.23929

differentiation of precursors in response to injury (Cramer and Chopp, 2000). These signaling pathways represent promising therapeutic targets to harness the potential of these precursors to enhance regeneration and repair.

The Notch pathway is an evolutionarily conserved mechanism for regulating cell fate decisions (Artavanis-Tsakonas et al., 1999). In mammals there are four homologues of the Notch receptor (Notch1-4). Signaling is mediated through cell–cell contact through the Delta-Serrate-Lag2 (DSL) family of type I transmembrane receptors. The mature Notch1 receptor consists of a furin-generated transmembrane protein with a relative molecular weight of ~120 kDa (Blaumueller et al., 1997). Upon ligand binding, Notch receptors undergo a series of cleavage events, culminating in the release of an ~80-kDa Notch intracellular domain (NICD) by γ-secretase (Schroeter et al., 1998; De Strooper et al., 1999; Kopan and Ilagan, 2009). In the canonical signaling pathway, NICD translocates to the nucleus and binds directly to CBF-1, Su(H), and LAG-1 (CSL), facilitating recruitment of the coactivator Mastermind and thus forming a transcriptional activation complex to regulate target genes including the Hairy/Enhancer of Split (Hes) family of basic helix-loop-helix (bHLH) transcription repressors (Mumm and Kopan, 2000; Friedmann et al., 2008). Additional evidence suggests that there are other noncanonical signaling pathways by which Notch functions independently of CSL (Sanalkumar et al., 2010; Jang et al., 2014).

Notch signaling is an important regulator of neural stem and progenitor cells (NSPs) both during development and in the adult brain, with pleiotropic effects on multiple aspects of NSP dynamics (Ables et al., 2011). It can influence NSP proliferation rates, with differential effects in vitro at high and low levels of activity, and oscillations of this activity may be crucial for maintenance of the neural progenitor pool (Guentchev and McKay, 2006; Shimojo et al., 2008). Multiple studies have demonstrated that Notch signaling can influence the symmetry of cell division and rates of self-renewal within NSP cultures (Chojnacki et al., 2003; Aguirre et al., 2010; Ferent et al., 2014). Interestingly, despite its necessity for maintaining the NSP population, Notch signaling does not appear to be essential for the initial establishment of the precursor pool as mice deficient in presenilin, the gene encoding γ-secretase, are born with normal numbers of NSPs but subsequently show a rapid decline in this population compared with wild-type mice (Hitoshi et al., 2002). In vivo Notch signaling also exhibits differential effects with temporal variation during the development of forebrain precursors (Chambers et al., 2001). In addition to effects on proliferation, Notch signaling can influence cellular identity and differentiation. Overexpressing active Notch1 in cortical precursors prior to embryonic neurogenesis promotes a radial glial phenotype, while overexpressing active Notch1 in early postnatal subventricular zone (SVZ) cells inhibits any differentiation and delays emergence from the SVZ (Chambers et al., 2001; Gaiano and Fishell, 2002).

Many studies have revealed the inherent plasticity of the brain, and increased neurogenesis is now well documented following brain injury (Romanko et al., 2004a). Ischemic injury, in particular, induces a strong proliferative response in the SVZ, a region of the brain known to harbor NSPs throughout life (Felling and Levison, 2003). Several years ago we showed that perinatal hypoxic–ischemic (H-I) brain injury stimulates proliferation of precursors within the SVZ prior to the peak of induced neurogenesis (Felling et al., 2006). These new precursors form tripotential, self-renewing neurospheres in vitro, indicating that the increase is relatively specific for the most undifferentiated precursors. In that study we provided evidence implicating Notch signaling, as it can influence neuroplasticity-related changes that occur in response to brain injury. Later studies of adult stroke observed that neurogenesis after stroke is dependent on Notch signaling (Androutsellis-Theotokis et al., 2006; Carlen et al., 2009; Shimada et al., 2012; Marumo et al., 2013; Sun et al., 2013). Similarly, hypoxia alone can induce Notch-dependent changes in neural precursors through direct interaction with hypoxia-inducible factor-1α (Gustafsson et al., 2005; Zhang et al., 2014). Given its importance in neurodevelopment and brain injury, Notch signaling is likely to play an influential role in the response to perinatal H-I.

Here we characterize the role of Notch1 in increasing NSPs following perinatal H-I. We present evidence of selective increases in Notch1 as well as one of its ligands, Delta-like 1, and its downstream effectors, Hes1 and Hes5. We further show that pharmacologically decreasing Notch1 activity during the acute recovery period in vivo abrogates the increase in NSPs. Finally, we show that H-I itself is not sufficient to induce Notch-1, but that it induces astrocytes to produce leukemia inhibitory factor (LIF), which in turn increases Notch1 expression in the NSPs. These results emphasize the importance of Notch1 signaling for the expansion of NSPs during recovery from brain injury. Thus, enhancing Notch signaling may be therapeutically beneficial in promoting regeneration from endogenous NSPs.

METHODS

Perinatal H-I Model

Animal experiments were in accordance with research guidelines set forth by the Society for Neuroscience Policy on the use of animals in neuroscience research. Timed pregnant Wistar rats (Charles River, Wilmington, DE) were fed high-fat lab chow (Harlan Teklad, Madison, WI). After normal delivery, the litter size was adjusted to 10 pups per litter. Cerebral H-I was produced in 6-day-old rats (day of birth being P0) by a permanent unilateral common carotid ligation followed by systemic hypoxia (Rice et al., 1981; Vannucci and Vannucci, 2005). Both male and female pups were used for all experiments. The pups were prewarmed for 20 min in jars submerged in a 37 °C water bath and then exposed to 1.5 hr of 8% O_2/92% N_2. After this

hypoxic interval, the pups were returned to their dam for recovery periods of 1, 2, and 3 days, at which time they were either decapitated for neurosphere assays or anesthetized and sacrificed by intracardiac perfusion for immunohistochemistry. Sham-operated animals were anesthetized, and the carotid was isolated from the vagus but not ligated. They were not subjected to a hypoxic interval. Control animals were separated from the dam for the same amount of time as experimental animals, but were otherwise not manipulated. In all cases, the contralateral and ipsilateral hemispheres from experimental animals were examined separately. The animal protocols for this work were approved by the Institutional Animal Care and Use Committees of either the Penn State College of Medicine or the New Jersey Medical School, which are both Association for Assessment and Accreditation of Laboratory Animal Care–accredited facilities.

DAPT Injections

P6 Wistar pups underwent common carotid ligation followed by systemic hypoxia with 8% O_2 at 37 °C. Animals were given subcutaneous injections with the compound at a dose of 10 mg/kg in a volume of 0.1 ml of 5% EtOH/0.3% DMSO in corn oil administered subcutaneously. Controls were injected with the vehicle. Animals were given 3 injections, 1 every 18 hr beginning 18 hr after the surgery. At 72 hr of recovery from surgery, pups were decapitated under sterile conditions, and the SVZs were isolated and dissociated as described below.

Digoxigenin In Situ Hybridization

Cryosections were thawed and postfixed for 15 min in 4% paraformaldehyde. After several rinses in phosphate buffer (PBT) with 0.1% Tween-20, they were treated with Proteinase K (1 μg/ml in PBT), then rinsed thoroughly in PBT followed by another postfix in 4% paraformaldehyde, further rinses, and treatment in 0.25% acetic anhydride in 100 mM triethanolamine. Sections were then rinsed and placed in humidified slide chambers and hybridized overnight at 65 °C in hybridization solution (10 mM Tris, 100 mM EDTA, 600 mM NaCl, 0.25% SDS, 10% dextran sulfate, 1X Denhardt's solution, 200 μg/ml yeast tRNA, and 50% formamide) with digoxigenin-labeled riboprobe against Hes5 generated according to manufacturer's instructions (Roche). Following hybridization, slides were rinsed in 5X SSC, then 1X SSC/50% formamide at 65 °C for 30 min, then treated with RNase (20 μg/ml) in TNE (10 mM Tris, 1 mM EDTA, 500 mM NaCl) for 30 min at 37 °C. Slides were then washed in 2X SSC and 0.2X SSC for 20 min each at 65 °C. Following two rinses in MABT (100 mM maleic acid, 150 mM NaCl, 0.1% Tween-20), sections were blocked with a 1:1 mixture of 10% Blocking Reagent (Roche) and Tris-buffered saline for 15 min. Sections were incubated overnight at 4 °C in alkaline phosphatase–conjugated anti-digoxigenin (Promega, 1:500) in blocking buffer. The following day, after thorough rinsing in MABT and preincubation with levamisole, sections were developed with NBT/BCIP.

Single-Molecule Fluorescent In Situ Hybridization

A set of 48 probes, each 20 nt long, was designed specifically to rat glial fibrillary acidic protein (GFAP) and rat LIF mRNA. The probes were ordered from LGC Biosearch, LLC with a 3′amino modification. The LIF probes were coupled with tetramethylrhodamine, whereas the GFAP probes were coupled with Texas Red. The coupled probes were then purified using HPLC (Batish et al., 2011). Sections from fresh frozen brains taken from H-I rats at 24 hr of recovery were sectioned at 10 μm and mounted onto poly-D-lysine–coated 12-mm-round coverslips. The sections were washed with 1X PBS, fixed using 4% paraformaldehyde, and permeabilized with 70% ethanol. A hybridization mix was prepared using 50 nM of each probe in a hybridization solution (containing 10% Dextran sulfate (w/v), 1 mg/ml *Escherichia coli* tRNA, 2 mM vanadyl ribonucleoside complex, 0.02% RNase free BSA, and 20% formamide). The sections were hybridized overnight at 37 °C. The coverslips were washed with wash buffer (20% Formamide in 2X SSC), at least four times each for 20 min, to remove unbound probes. The coverslips were mounted and sealed with transparent nail polish. Sections were imaged using a Nikon TiE inverted wide-field fluorescence microscope. Images were acquired at 100X using a cooled CCD Pixis camera interfaced to Metamorph imaging software. We acquired approximately 15 optical slices at 0.2-μm intervals, thereby covering the entire volume of the cells. The images were merged to composite and pseudo-colored using OpenLab Image processing software (Markey et al., 2014).

Neurosphere Quantitation

Neurospheres were produced as described previously (Felling et al., 2006). A neurosphere was defined as a free-floating, cohesive cluster of at least eight cells, although the vast majority of neurospheres ($>98\%$) were substantially larger than this. Plates were gently shaken before counting each well to ensure an even distribution of spheres. Ten random 10X fields were counted per well, and those performing the counting were blinded to the experimental group. The frequency of sphere-forming cells (i.e., NSPs) was calculated from the average number of spheres per field, the area of the field, and the area of the well. The number of NSPs per hemisphere was then extrapolated by applying the frequency of sphere-forming cells to the total number of cells obtained in the initial dissociation of the tissue.

Neurosphere Immunohistochemistry

Spheres were collected and resuspended in 5% horse serum in CNM-2 media (DMEM/F12 1:1 containing 10 ng/ml d-biotin, 5 ng/ml insulin, 20 nM progesterone, 100 μM putrescine, 5 ng/ml selenium, 50 μg/ml apo-transferrin, 50 μg/ml gentamicin, 150 μl of 0.5 M kynurenic acid) at an approximate density of 100 to 200 spheres per milliliter. One hundred microliters of the neurosphere suspension was then plated in plastic 24-well tissue culture plates onto flame-sterilized 12-mm coverslips precoated with 1% w/v poly-D-lysine and 10 μg/ml laminin. The spheres were allowed to attach in a 37 °C incubator for a minimum of 1.5 hr, after which 400 μl of CNM-2 supplemented to 5% horse serum was added to the well. After 16 to 20 hr, this media was replaced with CNM-2 with 0.03% DMSO. Cultures were allowed to differentiate for 5 days, with media replenished on day 3. After the differentiation period,

TABLE I. Antibody Characterization

Antibody name	Immunogen	Source	Dilution
Tuj1*	C-terminus of βIII tubulin (EAQGPK)	Promega, Cat #G7121 RRID: AB_430874 Mouse monoclonal IgG1	1:250
GFAP*	Full-length GFAP isolated from cow spinal cord	Dako, Cat #Z0334 RRID: AB_10013382 Rabbit polyclonal	1:200
O4*	Bovine white matter (pro-oligodendroblast antigen, sulfatide)	J. Salzer RRID: AB_2619717 Mouse monoclonal IgM	1:3
Notch1 (C-20)†	Human Notch1 C-terminus	Santa Cruz, Cat #sc-6014 RRID: AB_650336 Rabbit polyclonal	1:100
GAM IgG FITC (secondary)	Mouse IgG and Fc	MP Biomedicals, Cat #55508 RRID: AB_2334514 Goat polyclonal	1:400
GAR AMCA (secondary)	Rabbit IgG (H+L)	Jackson, Cat #111-155-003 RRID: AB_2337988 Goat polyclonal	1:200
GAM IgM LRSC (secondary)	Mouse IgM F(ab')2	Jackson, Cat #111-086-020 RRID: N/A Goat polyclonal	1:200
GAR HRP (secondary)	Rabbit IgG (H+L)	Jackson, Cat #111-035-144 RRID: AB_2307391 Goat polyclonal	1:10,000

*Tuj1, GFAP, O4: These primary antibodies have been extensively characterized in the literature. In the present experiments they were used solely for cell identification. Each antibody exclusively labeled cells with the expected morphology for their respective cell types.
†Notch1 (C-20): This antibody was characterized by Western blot, where it recognized a distinct banding pattern including bands at ~100 kDa and ~80 kDa corresponding to predicted sizes of the Notch1 transmembrane precursor and the cleaved Notch1 intracellular domain, respectively. Additionally, treatment with DAPT, an inhibitor of cleavage of the Notch1 intracellular domain, reduced the ratio of Notch intracellular domain precursor as expected. Commercially, specificity has been shown with a blocking protein corresponding to an epitope from the Notch1 C-terminus (sc-6014 P).

the cells were fixed using 2% paraformaldehyde for 15 min, and washed twice with BCH (10% bovine calf serum in Earle's basal medium with 4.8 mg/ml HEPES). Sections were stained at room temperature for 45 min with O4 culture supernatant (generated in our lab from O4 hybridoma cells, RRID: AB_2619717) diluted 1:3 in BCH supplemented with 10% lamb serum. After thoroughly rinsing, the cells were incubated for 45 min at room temperature in GAM IgM LRSC (Jackson Immunoresearch, West Grove, PA, cat #115-086-020, 1:200). The cells were then permeabilized with BCH-S (BCH with 0.5 mg/ml saponin) and stained for 45 min at room temperature with anti-βIII tubulin (Promega, cat #G7121, RRID: AB_430874, 1:250) and anti-GFAP (Dako, cat #Z0334, RRID: AB_10013382, Indianapolis, IN, 1:200) in saponin diluent (BCH-S supplemented with 10% lamb serum). Cells were then incubated for 45 min at room temperature in GAM IgG FITC (MP Biomedicals, 1:400, cat #55508, RRID: AB_2334514) and GAR AMCA (Jackson Immunoresearch, 1:200, RRID: AB_2337988) in saponin diluent. The coverslips were rinsed and mounted onto microscope slides with Gel/Mount (Biomeda, Foster City, CA) and allowed to dry overnight. Colonies were scored according to the types of cells present, and scorers were blinded to the experimental group. Images of stained cells were collected using a SenSys cooled–coupled device camera (CRI, Inc., Woburn, MA) interfaced with IP Lab scientific imaging software (Scanalytics, Fairfax, VA, RRID: SCR_002775) on an Olympus BX-40 microscope. Table I summarizes the antibodies that were used in these studies.

In Vitro Hypoxia–Hypoglycemia

P1 Wistar pups were sacrificed, and the brain was extracted under sterile culture conditions. The SVZ was isolated, and neurospheres were cultured as described above. The cortex and striatum were mechanically dissociated and subjected to enzymatic dissociation with trypsin at 37 °C for 30 min with gentle shaking. The enzymatic digestion was stopped with the addition of Minimal Essential Medium (MEM), supplemented with 0.6% dextrose, penicillin, and streptomycin). Tissue was triturated by passage through 10-ml pipette, and the supernatant was passed through a 130-μm filter. After another round of trituration, the suspension was passed through a 40-μm filter. Cells were plated in MEM-C at a density of 2×10^6 cells per well in 6-well culture plates to establish confluent beds of mixed brain cells. Media was changed every other day. After 4 DIV, experimental cultures were changed to DMEM-F12 without serum and placed in 2% O_2 for 3 hr. Control cultures received fresh media and were left in atmospheric culture conditions for this interval. After the hypoxia–hypoglycemia (H-H) interval, cells were rinsed once with DMEM-F12, and the media was changed to Pro-N+EGF/FGF-2. At this time, neurospheres that had been established simultaneously at P1 were placed into Transwells (Corning, Corning, NY) and cultured in the same wells with either experimental or control mixed brain cells for an additional 3 days in a biochemically defined culture medium (Pro-N) supplemented with 20 ng/mL epidermal growth factor (EGF) and 10 ng/mL fibroblast growth factor-2 (FGF-2). Separate neurosphere cultures were also subjected to the in vitro H-H paradigm at the same time as the mixed brain cells. These neurosphere cultures were returned to their normal culture conditions following the H-H interval for an additional 3 days.

Western Blot

The cortex and striatum were isolated from control and experimental animals and homogenized in lysis buffer (20 mM

TABLE II. Primers Used for Quantitative Polymerase Chain Reaction

Transcript	Primers
Hes1	Applied Biosystems TaqMan Assay ID Rn00577566_m1
Hes5	Applied Biosystems TaqMan Assay ID Rn00821207_g1
Nov/CCN-3	5′-GAA CCA ACA GAC TCG TCT CTG CAT GG TC-3′ 5′-AGG TGG ATG GAT TTC AGG GAC T-3′
Jagged1	5′-GAA CTG GCT CCG CCG CAA CAG TC-3′ 5′-CAT GCA GAA CGT GAA CGG AGA-3′
Jagged2	5′-CAC GGA AGG AGT GCA AAG AAG CCG G-3′ 5′-CCC GTG GAG CAA ATT ACA TCC T-3′
Delta-like 1	5′-GTA CCT CAG GGC TGC TGG CAG GAC-3′ 5′-GGC CGC TAC TGC GAT GAA T-3′
Notch1 (Lux)	5′-CAC GTA CTG CGA GCT GCC CTA CGG-3′ 5′-GGC AGG TGC CTC CGT TCT-3′
18S (TaqMan)	Applied Biosystems TaqMan Assay ID Hs99999901_s1
18S (Lux)	Invitrogen Cat #115HM-01

Tris, 150 mM NaCl, 1 mM EDTA, 1 mM EGTA, 1% Triton X-100, 2.5 mM sodium pyrophosphate, 1 mM glycerophosphate, 1 mM sodium orthovanadate) with protease inhibitor cocktail (Sigma, St. Louis, MO) by mechanical shearing through a 25-gauge syringe followed by sonication. Protein concentrations were calculated using a standard BCA assay according to the manufacturer's instructions (Pierce, Rockford, IL) prior to Western blot analysis. Thirty microliters of protein sample was combined with 4X NuPage LDS sample buffer and 10X NuPage reducing agent, heated at 70 °C for 10 min, and loaded onto a NuPage 7% Tris-Acetate precast gel (Invitrogen, Carlsbad, CA). Standard lanes were loaded with 5 μL MagicMark XP (Invitrogen) and Kaleidoscope (Bio-Rad, Hercules, CA) molecular weight standards. After gel electrophoresis, proteins were transferred to nitrocellulose and stained with Ponceau-S to evaluate total protein. The blots were rinsed and incubated overnight at 4 °C with gentle shaking with polyclonal antibody to Notch1 C-terminus (Santa Cruz, sc-6014, 1:100). After three rinses in PBS-Tween, they were incubated with HRP-conjugated secondary antibody for 2 hr at room temperature with gentle shaking. The blots were exposed with Western Lightning chemiluminescence reagent according to manufacturer's instructions (PerkinElmer, Wellesley, MA). Images were captured in a UVP EpiChem^3 darkroom and processed using Labworks 4.0 digital quantification software (UVP, Upland, CA).

RNA Isolation

SVZs were dissected out of control and the ipsilateral hemisphere of H-I animals and snap frozen on a dry ice/ethanol slush and immediately stored at −80 °C. Dissections were directed toward the angles of the ventricles to avoid any confounding effects of ventricular hypertrophy due to striatal degeneration. Tissue samples were then thawed directly into 0.5 ml Trizol reagent (Molecular Research Center, Cincinnati, OH) and homogenized using a tissue homogenizer. One hundred microliters of chloroform was added, and the samples were centrifuged at 13,000 rpm for 15 min at 4 °C. The aqueous phase was then transferred to a new tube. After adding 250 μl of 70% EtOH, the aqueous phase was applied to an RNeasy Mini-spin column (Qiagen, Valencia, CA) to remove contaminants from the RNA, according to manufacturer's instructions. The concentration of total RNA was determined by measuring optical density on a spectrophotometer (Becton-Dickson, Franklin Lakes, NJ). RNA samples were stored at −80 °C until needed.

Quantitative Polymerase Chain Reaction

Two micrograms of total RNA was reverse transcribed to cDNA using the Qiagen Omniscript RT kit supplemented with random nonamer primer (Sigma Aldrich, St. Louis, MO) and RNaseIN (Promega, Madison, WI). Primer pairs specific for the genes of interest were designed using Lux Primer Design software (Invitrogen, Carlsbad, CA) or obtained from catalogued TaqMan gene expression assays (Applied Biosystems, Foster, City, CA) (Table II). Amplification was carried out in 96-well plates using Platinum-UDP Supermix kit according to the manufacturer's instructions (Invitrogen, Carlsbad, CA) and analyzed on an ABI Prism 7700 Sequence Detection System (Applied Biosystems, Foster City, CA).

Statistical Analysis

In these studies, litters were culled to 12 pups per dam, and all of the pups were used. There were no outliers excluded from the statistical analyses. In any experiment in which the data points were manually obtained (i.e., neurosphere clone counting), the analysts were blinded to the condition. For experiments with continuous variables, results were analyzed for statistical significance using Student *t*-test. For experiments with categorical variables (differentiation comparisons), the distributions were compared using chi-square test for independence, with post hoc pairwise comparisons of significant results using *t*-tests with Bonferroni correction for multiple comparisons. Comparisons were interpreted as significant at $P < 0.05$. Analysis of variance (ANOVA) with post hoc Tukey honest significant difference was used to analyze experiments with multiple group comparisons. All data are expressed as mean ± SEM. For in vivo studies, at least three animals were examined per group at each time point. For in vitro studies, three to six samples were analyzed for each experiment and were repeated at least twice. Fold changes in gene expression relative to a housekeeping gene were obtained using the Relative Expression Software Tool for groupwise comparison and statistical analysis of relative expression results in quantitative polymerase chain reaction (qPCR; Pfaffl et al., 2002). This algorithm provides a *P* value based on the pairwise fixed reallocation randomization test.

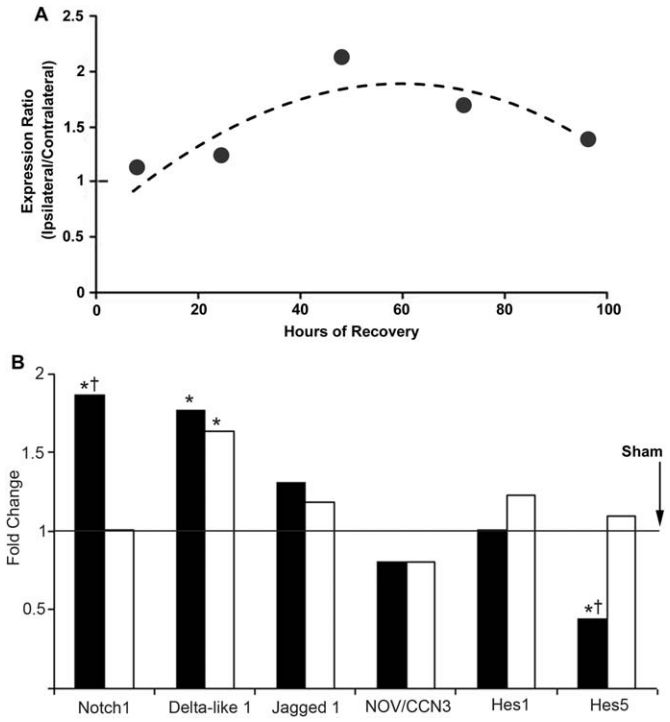

Fig. 1. Components of the Notch signaling pathway are induced following perinatal hypoxia–ischemia (H-I). **A**: Notch1 expression was analyzed by quantitative polymerase chain reaction (qPCR) from ipsilateral (circles) and contralateral (solid line) subventricular zones (SVZs) at time points between 8 and 96 hr after H-I. $n = 3$ animals per group per time point. **B**: Notch signaling components were analyzed by qPCR from ipsilateral (solid bars), contralateral (white bars), and sham (solid line) SVZs 48 hr following perinatal H-I. $n = 10$ (HI), $n = 4$ (sham). $^{\star}P < 0.05$ vs. sham; $^{\dagger}P < 0.05$ vs. contralateral by Relative Expression Software Tool.

RESULTS

Notch1 and Delta Expression Increase within the First 2 days of Recovery from Perinatal H-I

In a microarray analysis we found increased expression of Notch1 within the SVZ 2 days following perinatal H-I (Felling et al., 2006). To determine the time course of Notch1 induction, we microdissected the SVZ from the ipsilateral and contralateral hemispheres of H-I animals as well as from sham-operated controls and performed qPCR to assess the expression of Notch1 mRNA as well as several Notch ligands. This analysis revealed that Notch1 expression peaked at 48 hr after H-I at approximately twofold compared with the contralateral hemisphere. Notch1 mRNA then decreased over the next 48 hr towards levels observed in the contralateral hemisphere (Fig. 1A). Expression in the contralateral hemisphere at 48 hr of recovery was comparable to expression in sham-operated controls (Fig. 1B). An important Notch ligand, Delta-like 1, showed a similar increase in expression in the ipsilateral hemisphere at 48 hr, but its expression was almost equally increased in the contralateral hemisphere. Other Notch ligands, Jagged-1 and Nov/CCN3, remain unchanged in either hemisphere at 48 hr of recovery. Similarly, Hes1, a downstream target of Notch signaling, was unchanged compared with sham-operated animals, and Hes5, another downstream target, was reduced when expression in the entire SVZ of the ipsilateral hemisphere was compared with the contralateral hemisphere or a sham-operated control.

In situ hybridization revealed regional differences in the expression of these Notch pathway components within the SVZ. This analysis revealed that Notch1 mRNA was particularly induced within the most medial aspect of the SVZ, just subjacent to the ependymal layer (Fig. 2A). Both control and contralateral hemispheres exhibited comparably homogeneous expression throughout the SVZ (Fig. 2B, C). This pattern of higher expression in the medial SVZ with normal or decreased expression throughout the remainder of the SVZ also occurred for the ligands Delta-like 1 (Fig. 2D–F) and Jagged-1 (Fig. 2G–I). Whereas our measures of Hes5 mRNA revealed a decrease when the entire SVZ was analyzed by qPCR, Hes5 mRNA was induced in the same regions where Notch1 and Delta-like 1 were increased (Felling et al., 2006).

Pharmacologically Inhibiting Notch1 In Vivo Reduces the Increase in NSPs following Perinatal H-I

To determine whether Notch signaling is essential for the increase in NSPs after perinatal H-I, we administered a commercial γ-secretase inhibitor (DAPT) by subcutaneous injection and then analyzed the number of NSPs using the neurosphere assay and also assessed their differentiation potential. We used a γ-secretase inhibitor, as this is the enzyme responsible for the final cleavage event that releases the active NICD (De Strooper et al., 1999). We administered three doses of the inhibitor every 18 hr beginning 18 hr after perinatal H-I. Previous experiments had demonstrated persistent levels of compound in excess of the in vitro LD50 within brain tissue up to 18 hr following this route of administration (Dovey et al., 2001). Western blotting for Notch1 protein revealed a decrease in the ratio of the NICD fragment (80 kDa) to its immediate precursor (100 kDa) following injection of the inhibitor compared with vehicle (Fig. 3A, 0.13 DAPT vs. 0.24 vehicle, $P = 0.01$). Following vehicle alone, the ipsilateral hemisphere yielded > 50% more neurospheres than the contralateral hemisphere, as we have shown previously. However, the expansion of the NSPs decreased to the same extent that Notch1 processing was inhibited following DAPT administration. Almost equivalent numbers of neurospheres were obtained from the contralateral and DAPT-treated ipsilateral hemispheres 3 days following perinatal H-I (Fig. 3B).

To further elucidate the effect of DAPT administration on the NSPs, we differentiated six DIV primary neurospheres from ipsilateral hemispheres of vehicle- and DAPT-injected pups. The progeny of each neurosphere

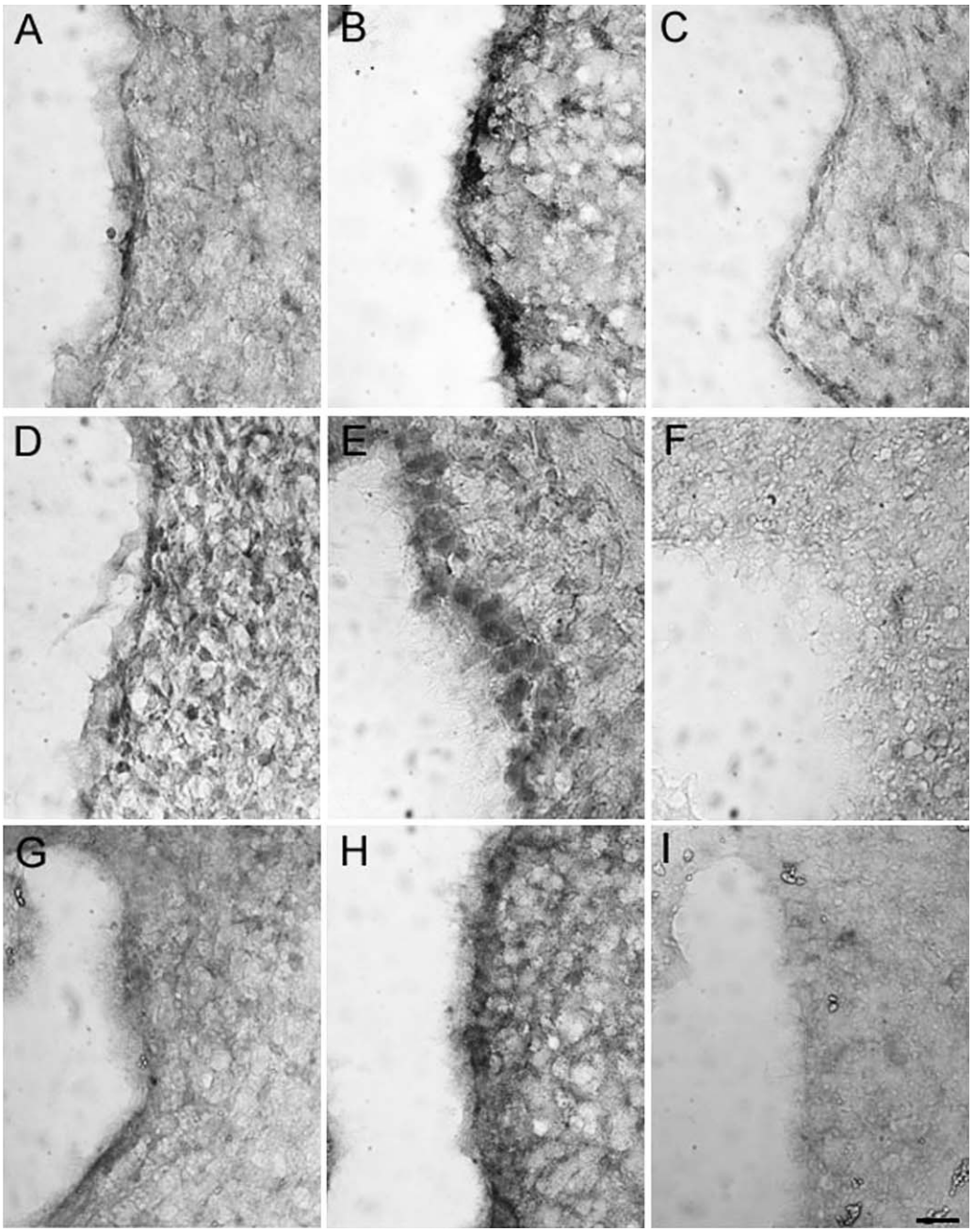

Fig. 2. Notch1 receptor and its ligands are induced within the neural stem/progenitor niche following perinatal hypoxia–ischemia. Nonradioactive in situ hybridizations were performed on cryostat sections of contralateral (**A, D, G**), ipsilateral (**B, E, H**), and control (**C, F, I**) hemispheres using digoxigenin-labeled RNA probes for Notch1 (**A–C**), Delta-like 1 (**D–F**), or Jagged-1 (**G–I**). Scale bar in **panel I** represents 10 μm.

were stained for neural cell lineage markers (GFAP, O4, and Tuj1), and the colonies were scored according to the combinations of cells present. In the vehicle-injected animals, ~80% of the neurospheres produced neurons, oligodendrocytes, and astrocytes compared with ~30% from the DAPT-injected animals (Fig. 3 C, D).

Mixed Brain Cells Subjected to H-I In Vitro Are Required to Stimulate the Proliferation of Neurospheres

Neurospheres generated from the injured brain grow faster in vitro than spheres generated from an undamaged brain. We developed an in vitro model to

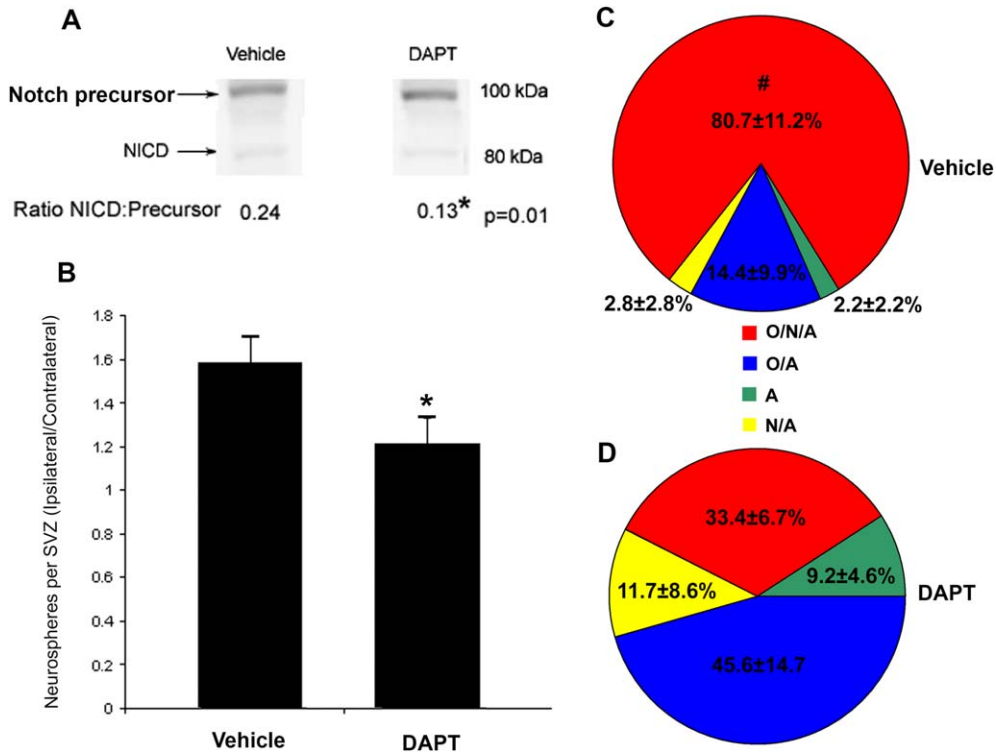

Fig. 3. Inhibiting Notch activity reduces the expansion of neural stem and progenitor cells following perinatal hypoxia–ischemia (H-I). DAPT, a γ-secretase inhibitor, was administered subcutaneously during the first 3 days of recovery from perinatal H-I. **A**: Western blots were performed using an antibody to Notch1 that recognized both the full-length protein as well as the γ-secretase–cleaved Notch intracellular domain (NICD). **B**: Neurosphere assays were performed upon completing DAPT administration, and the ratio of neurospheres generated from the ipsilateral to the contralateral hemisphere was calculated, $n = 10$ DAPT, 9 vehicle, $\star P < 0.05$ by Student *t*-test, DAPT vs. vehicle. After maintaining the neurospheres for 6 DIV, spheres from the ipsilateral subventricular zone (SVZ) for either vehicle-treated (**C**) or DAPT-treated (**D**) animals were plated onto coverslips and differentiated for 4 DIV, after which they were stained for GFAP (astrocytes), O4 (oligodendrocytes), and class III beta tubulin (neurons). Colonies were scored according to which cell types they possessed, $n = 3$ animals per group, $\#P < 0.01$ by *t*-test with Bonferroni correction for multiple comparisons following chi-square test for independence.

determine whether these proliferative changes following perinatal H-I are due to a direct effect of H-I on the NSPs. Neurospheres were established in EGF-supplemented medium for 3 DIV, after which they were resuspended in medium with low glucose (0.15 mM) and no growth factors and cultured for 3 hr in 3% O_2 (Fig. 4A). After this H-H episode, which we have previously used to model in vivo H-I (Alagappan et al., 2013), they were returned to normal neurosphere medium supplemented with EGF and to a conventional cell culture incubator. A 24-hr pulse of ^{3}H-thymidine was given on days 1, 2, or 3 following the H-H exposure. At days 1 and 2 of recovery, neurospheres exposed to in vitro H-H only incorporated ~50% as much ^{3}H-thymidine as control cultures. By 3 days of recovery, there was no significant difference in the level of thymidine incorporation (Fig. 4B).

Mixed Brain Cells Subjected to H-I In Vitro Express LIF and Stimulate Notch1 Expression in Neurospheres

A second strategy was implemented to determine whether signals derived from more mature cells surrounding the NSP niche were responsible for altering their expansion. Mixed brain cell cultures were prepared from neonatal rat cerebral cortices and cultured in parallel to the neurosphere cultures for 3 DIV, after which the mixed brain cells were exposed to the in vitro H-H paradigm described above. The mixed brain cells were then returned to atmospheric culture conditions. Neurospheres, which had never been exposed to in vitro H-H, were then placed into Transwells and cultured suspended above either those mixed brain cells subjected to H-H or to control mixed brain cells. After 2 days of co-culture, ^{3}H-thymidine was added for 24 hr to evaluate cell proliferation. Under these circumstances, the NSPs incorporated more ^{3}H-thymidine when exposed to the H-I mixed brain cells than when they were exposed to control cultures (Fig. 4C). Under these same conditions, Notch1 mRNA expression was increased 1.5-fold (Fig. 5A).

We previously established that LIF expression increases after H-I and that LIF can induce Notch1 (Covey and Levison, 2007). Therefore, it was of interest to establish whether H-I itself could induce Notch1 or whether the expression of Notch1 might be induced

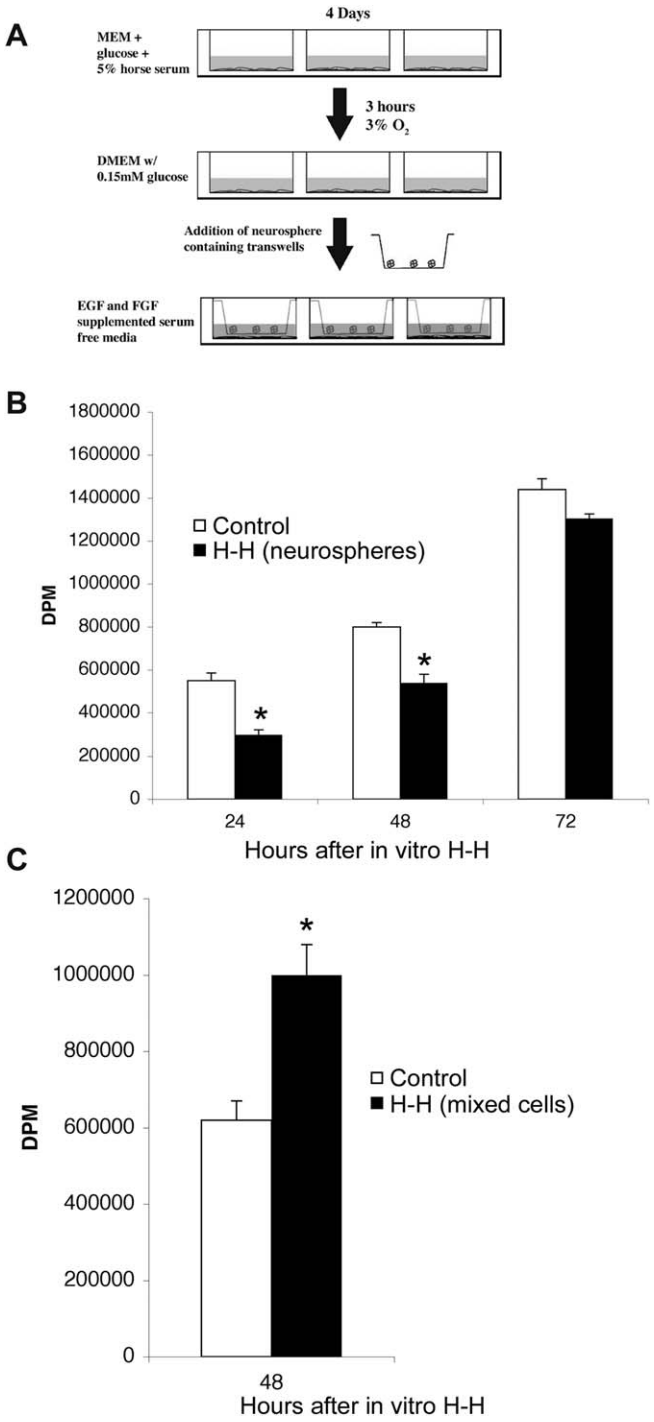

Fig. 4. Neural stem and progenitor cells respond to paracrine signals following hypoxia–hypoglycemia (H-H). **A**: Schematic of the co-culture paradigm. **B**: Neurospheres were subjected to in vitro H-H, and ^{3}H-thymidine incorporation was quantified. $P < 0.001$ by ANOVA, but Ctl (white bars) vs. H-H (black bars) was not significant at any time point with post hoc Tukey honest significant difference. **C**: Neurospheres were placed into Transwells and exposed to medium from mixed brain cells that had been exposed to in vitro H-H, and ^{3}H-thymidine incorporation was measured during the final 24 hr. $n = 6$, $\star P \leq 0.005$ vs. control by Student *t*-test.

subsequent to the induced expression of LIF. To test the hypothesis that H-I was directly inducing Notch1 expression, we exposed NSPs to H-H. In the same experiment we exposed confluent beds of mixed brain cells to in vitro H-H, and qPCR for Notch1 was performed. Consistent with the proliferation results, Notch1 expression was not induced within neurospheres subjected to the in vitro H-H paradigm alone (Fig. 5A), but the mixed glial cells exposed to H-H induced Notch1. In a similar experiment, mixed brain cells were exposed to 3 hr of H-H, and mRNA was analyzed at 6, 12, or 24 hr of recovery. This analysis revealed a significant increase in LIF mRNA expression relative to 18S at all three time points vs. control, but there were no statistical differences in the relative levels of LIF between these time points ($P > 0.05$ by one-way ANOVA). LIF was induced 8- to 11-fold in these mixed brain cell cultures compared with cultures maintained under standard culture conditions. Maximal expression was observed at 12 hr of recovery (Fig. 5B; $F_{3,12} = 9.4$; $n = 4$; $P < 0.005$).

The mixed brain cell cultures contain astrocytes, oligodendrocytes, and microglial cells, and we hypothesized that the astrocytes were the source of the LIF. To test this hypothesis, neurospheres were established, and after 3 days they were placed in Transwells for 3 days with mixed brain cell cultures or enriched astrocyte cultures previously exposed to in vitro H-H or maintained under standard culture conditions, and Notch1 expression was analyzed. Again, we obtained a twofold increase in Notch1 expression when the NSPs were maintained with either the mixed brain cells or the astrocytes exposed to H-H (Fig. 5C). To demonstrate that the astrocytes were indeed the source of LIF, we compared the amount of LIF produced by the H-H astrocytes compared with NSPs. As shown in Figure 5D, astrocytes exposed to H-H produced ~500 pg/ml of LIF over 48 hr, whereas LIF was undetectable in the culture medium from the NSPs.

Finally, we wanted to establish whether the astrocytes in the SVZ were producing LIF in response to perinatal H-I. For these studies, we performed in situ hybridization using digoxigenin-labeled probes and ^{35}S-labeled probes combined with immunofluorescence for GFAP. However, despite repeated trials, a signal for LIF could not be detected above background. Therefore, we used single-molecule fluorescent in situ hybridization (smFISH), which has been used successfully in vitro to detect single molecules of mRNA, but has not been used extensively on tissue sections (Batish et al., 2011; Markey et al., 2014). Sections were hybridized with probes for both LIF and GFAP coupled to different fluorophores. With this method, the RNAs appear as diffraction-limited spots in a fluorescence microscope. As shown in Figure 6, the levels of both GFAP and LIF mRNAs increased in the ipsilateral (Figs. 6A, C, E) compared with the contralateral hemisphere (Figs. 6B, D, F), with the most robust expression of LIF present within the ipsilateral SVZ (Fig. 6A), intermediate levels in the striatum (Fig. 6C), and relatively low levels of LIF mRNA expressed in the neocortex (Fig. 6D). The SVZ cells that expressed high levels of

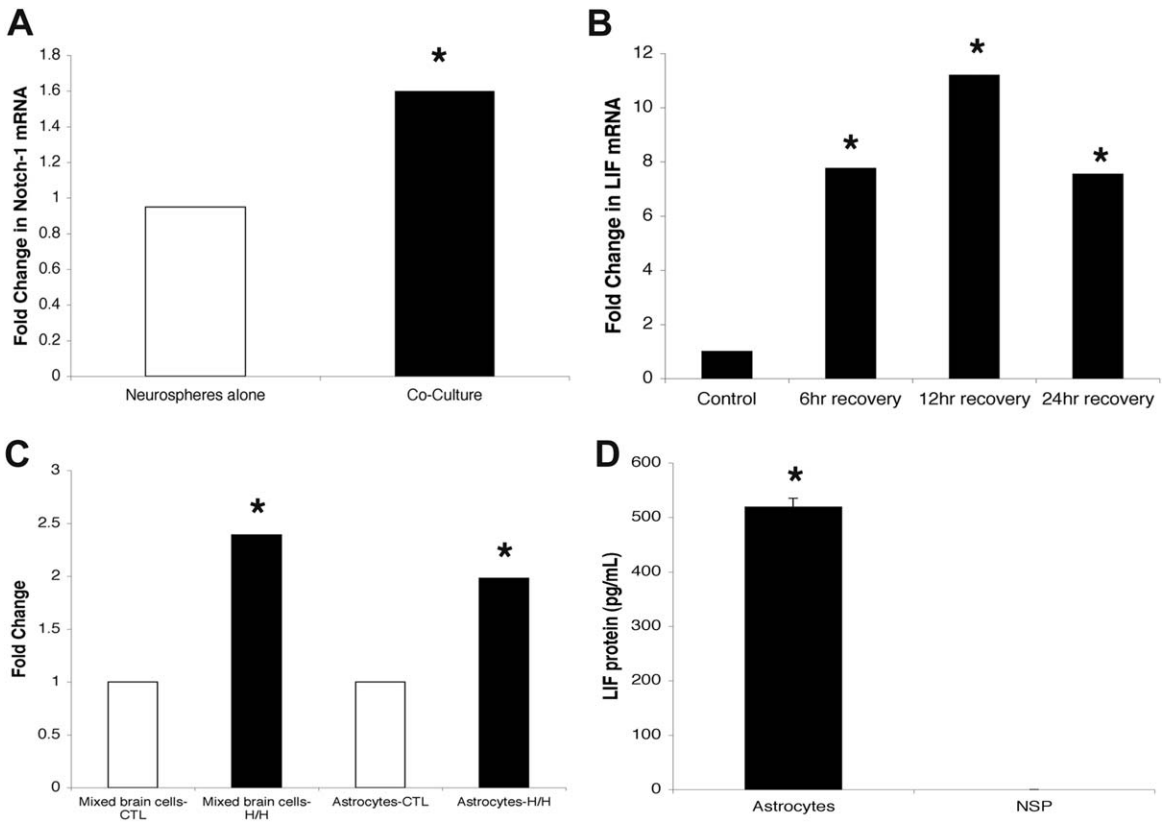

Fig. 5. Paracrine signals induce Notch1 in neural stem and progenitor cells (NSPs). **A**: Neurospheres were exposed to in vitro hypoxia–hypoglycemia (H-H) (neurospheres alone) or cultured with mixed brain cells that had been exposed to in vitro H-H (co-culture). RNA was isolated after 48 hr, and Notch1 mRNA was quantified by quantitative polymerase chain reaction (qPCR). **B**: Mixed brain cell cultures were exposed to H-H in vitro for 3 hr and then allowed to recover in an atmospheric incubator for 6, 12, or 24 hr. Leukemia inhibitory factor (LIF) expression was analyzed by qPCR. **C**: Mixed brain cell cultures were exposed to H-H as in **panel B**. Astrocyte cultures were similarly exposed to H-H in vitro, and LIF expression was analyzed by qPCR. **D**: LIF protein from cultured astrocytes and cultured NSPs was measured by enzyme-linked immunosorbent assay at 48 hr after H-H. $n = 6$ per group. $^{*}P < 0.05$ by Student *t*-test.

LIF mRNA also expressed GFAP mRNA, and the majority of these double-positive cells resided within or adjacent to the neural stem cell niche. We did not observe any GFAP + cells whose nuclei were adjacent to ventricles that contained LIF mRNA fluorescent dots.

DISCUSSION

Notch-DSL signaling regulates stem and progenitor cell populations both during development and in the mature brain (Imayoshi et al., 2010). Here we present evidence that Notch signaling participates in the regenerative response to developmental brain injury. We previously demonstrated that perinatal H-I expands the NSP population in the SVZ through increased proliferation and a shift in the mode of cell division (Felling et al., 2006). Most recently, we established that LIF is a key regulator for a subset of NSPs that expand during acute recovery from neonatal H-I (Buono et al., 2015). Here, we demonstrate that this expansion is preceded by an upregulation of Notch1 receptor and Delta-like 1 expression. The signaling molecules are not uniformly induced by neural precursors but are selectively increased in the most medial cell layers of the SVZ, where the stem cells and most primitive progenitors are known to reside. Inhibiting Notch activation in vivo during the acute recovery period reduced Notch1 activation and diminished the NSP expansion. Finally, we have established that the induction of Notch1 is not a cell-autonomous response but, rather, occurs as a consequence of LIF production by cells within the stem cell niche.

Notch1 expression peaked in the ipsilateral SVZ 48 hr following perinatal H-I. At this time point, the contralateral hemisphere exhibited no difference in Notch1 expression relative to a sham-operated control. In our animal model the contralateral hemisphere is uninjured, but it is exposed to systemic hypoxia. This result indicates that brief hypoxia alone is insufficient to induce Notch1 expression, suggesting that the induction observed following perinatal H-I is the result of injury signals produced from cells either surrounding the neural stem cell niche or within the cells themselves. This premise is supported by the observations that GFAP + SVZ astrocytes had high

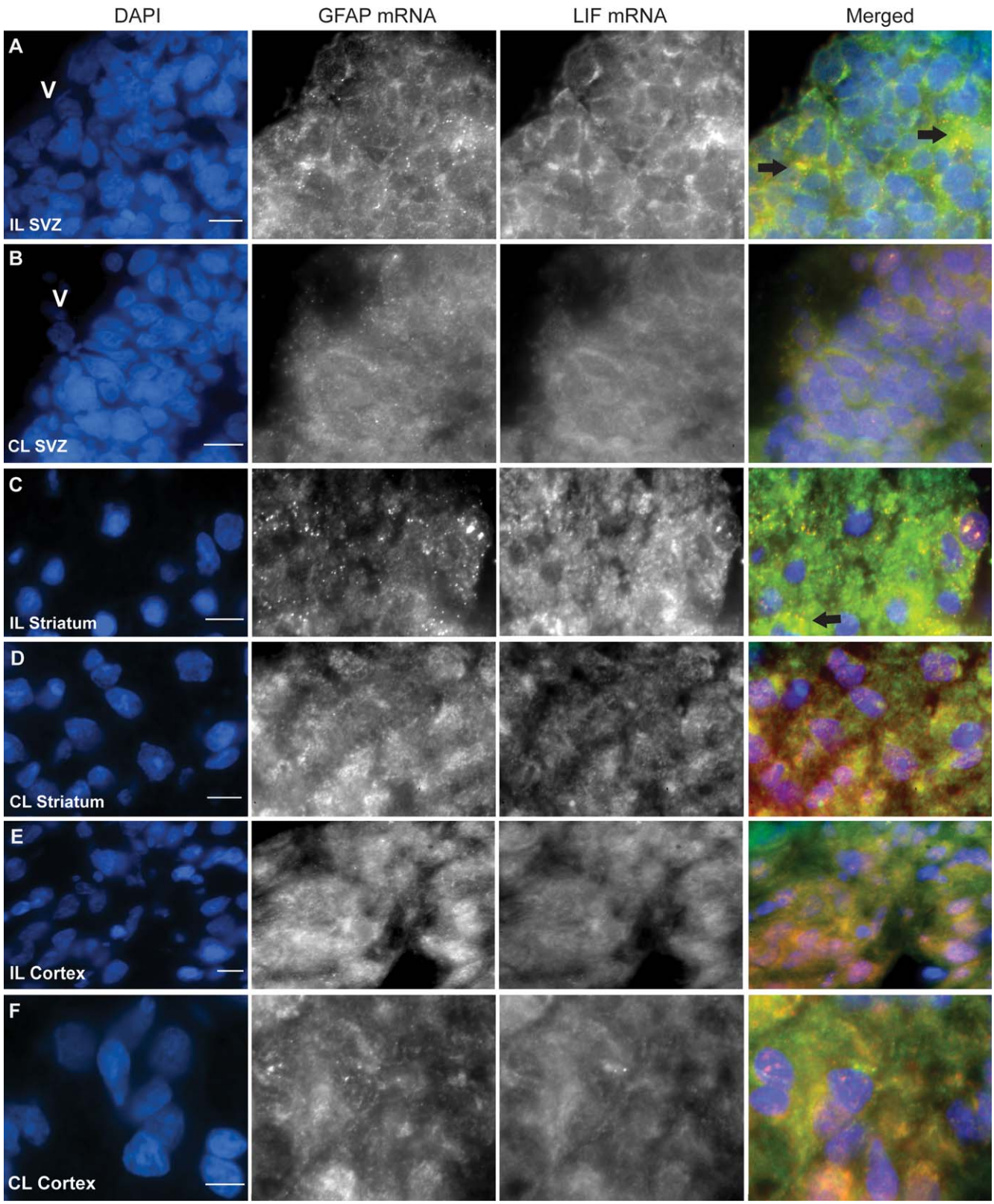

Fig. 6. Leukemia inhibitory factor (LIF) expression increases in astrocytes after perinatal hypoxia–ischemia (H-I). Single-molecule fluorescent in situ hybridization imaging was performed on 10-μm cryostat sections of ipsilateral (IL) (**A, C, E**) and contralateral (CL) (**B, D, F**) hemispheres at 24 hr after perinatal H-I. Sections depict pseudo-colored DAPI-stained images (column 1), GFAP mRNA using probes labeled with Texas Red (column 2), LIF RNA using probes labeled with tetramethylrhodamine (column 3), and a merged image where LIF dots are pseudo-colored green, GFAP dots pseudo-colored red, and DAPI-stained nuclei pseudo-colored blue (column 4). Panels **A** and **B** depict the ipsilateral and contralateral subventricular zone (SVZ), **panels C** and **D** depict the ipsilateral and contralateral striatum, and **panels E** and **F** depict the ipsilateral and contralateral neocortex. V represents the lateral ventricle in **panels A** and **B**. Arrows denote double-positive cells. The scale bars represent 5 μm.

levels of LIF mRNA after perinatal H-I and that astrocytes exposed to in vitro H-H released LIF into the culture medium, and they induced Notch1 in NSPs subsequently co-cultured with them. Consistent with these results, Notch1 was not induced in NSPs exposed to in vitro H-H. Delta-like 1, on the other hand, was equally induced both in the ipsilateral and contralateral hemispheres, suggesting that brief exposure to hypoxia induces this Notch ligand.

Other components of the Notch signaling pathway were not changed as robustly as Notch1, Delta-like 1, or Hes5. Rather, they appeared to be reduced throughout most of the SVZ, with maintained or increased expression in the most medial cells of the region. Importantly, the medial SVZ provides the niche for NSPs (Garcia-Verdugo et al., 1998). This region remains relatively undamaged following perinatal H-I, allowing it to remain capable of responding to injury signals from the surrounding damaged tissue (Romanko et al., 2004b).

Notch receptors play important regulatory roles in cell fate decisions in many tissues, both during development and in adulthood. In the brain, Notch1 is essential to maintaining the neural stem cell population by promoting self-renewal (Imayoshi et al., 2010; Basak et al., 2012). Mice deficient in *Notch1* or other pathway components, including *presenilin* (γ-secretase) or *RBP-Jκ*, exhibit a progressive loss of NSPs (Gao et al., 2009; Ehm et al., 2010; Imayoshi et al., 2010; Basak et al., 2012; Wang et al., 2016). This defect can be rescued with the introduction of activated Notch1 (Hitoshi et al., 2002). Inhibiting Notch activity in neurospheres in vitro, either pharmacologically or genetically, also reduces the self-renewal capacity of NSPs to generate secondary neurospheres (Chojnacki et al., 2003).

Our data demonstrate a similar role for Notch in the acute expansion of the NSP population following perinatal H-I because inhibiting Notch signaling eliminates this expansion. Interestingly, the level of Notch inhibition achieved in these studies is insufficient to appreciably reduce the number of NSPs in the normal brain, but it produces a significant reduction in the number of new NSPs generated in response to the injury. One reason for this could be the length of treatment. In the normal adult SVZ, NSCs are a slowly dividing population with a cell cycle time estimated at 15 days (Morshead et al., 1994). In our experiments, the inhibitor was only present in the brain for 48 hr prior to sacrifice, making it unlikely that it would have an appreciable effect on the numbers of existing NSCs. Following H-I, however, we have shown a doubling in their numbers; therefore, our data suggest that Notch1 is required for the expansion in the numbers of NSPs that would normally occur post injury.

Studies in both adult and neonatal stroke have shown that Notch participates in neurogenesis after stroke (Androutsellis-Theotokis et al., 2006; Carlen et al., 2009; Shimada et al., 2012; Marumo et al., 2013; Sun et al., 2013). Other studies have shown that inhibiting Notch1 signaling with a γ-secretase inhibitor reduces damage and improves functional outcome (Arumugam et al., 2006, 2011; Baik et al., 2015). Interestingly, these studies showed that in the acute recovery period, Notch signaling enhances apoptotic signaling cascades leading to neuronal death. One possibility for the apparently divergent results is offered by a study showing that different levels of active Notch1 can alter the specific cellular responses to Notch signaling (Guentchev and McKay, 2006). Additionally, it may be that temporal variation exists in the effects of Notch signaling as the neural stem cell niche transitions from an injury phase into a recovery phase. Further investigations are necessary to clarify these differential effects on cell death and regeneration.

The effects of Notch signaling on NSPs are principally mediated by the bHLH transcription factors, *Hes1* and *Hes5* (Ohtsuka et al., 2001; Kageyama et al., 2005). While deficiency in either of these genes alone leads to compensatory expression of the other, deficiency in both of these genes leads to disorganized neural tube formation and premature neuronal differentiation of neuroepithelial precursors at the expense of astrocytes and oligodendrocytes (Kageyama et al., 2005). Overexpression of Hes1, on the other hand, promotes astrogliogenesis (Wu et al., 2003). Furthermore, *Hes1*$^{-/-}$*;Hes5*$^{-/-}$ mutants exhibit reduced ability to generate neurospheres, although the few spheres that do form are still multipotential (Ohtsuka et al., 2001). Consistent with these data, we reduced the expansion of NSPs following perinatal H-I, a process likely related to the self-renewal of these cells, by pharmacologically inhibiting Notch. In contrast, however, inhibiting Notch in our studies compromised the multipotentiality of the resulting neurospheres. This difference is likely a distinction between the embryonic neuroepithelial precursors analyzed in the *Hes1*$^{-/-}$*;Hes5*$^{-/-}$ mice and the postnatal NSPs present in our studies, although our data might be indicating a Hes-independent function of Notch. Alternatively, the difference could be an effect of the relative "dose" of Notch signaling as described previously. Studies on these knockout mice would be informative; however, such studies would be predicated on the assumption that the NSP expansion and the mechanisms that regulate their expansion are conserved across species. Contradicting this assumption, rat SVZ cells increase in number after neocortical injury, whereas mouse SVZ cells do not (Szele and Chesselet, 1996; Goings et al., 2004). Indeed, our studies on the responses of mouse SVZ cells to H-I suggest differences in the NSP response compared with the results obtained in immature rats (Buono et al., 2015); therefore, additional studies will be required prior to initiating studies using mouse knockouts of the canonical Notch signaling pathway proteins.

A concern with the use of DAPT is that γ-secretases are involved in other functions in the brain besides Notch cleavage, most notably the processing of amyloid precursor protein (APP) (Carroll and Li, 2016). This leaves the possibility that the effect of the inhibitor that we have seen is due not to decreased Notch activity but, rather, to altered APP processing. In fact, a study has shown that the soluble form of APP (sAPP), generated mostly through cleavage by an α-secretase, actually stimulates

proliferation of cells within the SVZ (Caille et al., 2004). By inhibiting γ-secretase, we would expect a larger amount of APP to be processed via the alpha cleavage, thus generating more sAPP and stimulating proliferation within the SVZ. Rather, we see a *decrease* in these precursors with the inhibition of γ-secretase, suggesting that our results are not due to altered processing of APP.

Using the in vitro H-H insult paradigm, we demonstrate that NSPs require signals from their environment to stimulate their proliferation and to upregulate their expression of Notch1. NSPs exposed to in vitro H-H did not exhibit increased rates of proliferation in contrast to what we have previously observed from NSPs exposed to H-H in vivo. However, the increased proliferation of NSPs co-cultured in Transwells with mixed brain cells exposed to in vitro H-H, measured by thymidine incorporation, suggests that factors from the other cells found in the stem cell niche are required to initiate the NSP response to H-I. In Transwells, the neurospheres were never in contact with the mixed brain cells, indicating that a diffusible factor is responsible for this effect. One candidate molecule is LIF. LIF signals through a receptor complex that includes gp130, a protein that appears to regulate the expression of Notch1 (Chojnacki et al., 2003). Our laboratory has shown that LIF increases following perinatal H-I (Covey and Levison, 2007; Buono et al., 2015), the timing of which coincides with the increase in Notch1 induction. Here we have established that LIF increases Notch1 and Delta-like 1 expression in vitro in NSPs. Since astrocytes are the major source of LIF in the central nervous system (Ishibashi et al., 2006), we hypothesized that H-I would stimulate the astrocytes surrounding the NSPs to produce LIF, and, as shown in Figure 5, cultured astrocytes exposed to H-H did indeed increase their production of LIF. By contrast, LIF production was undetectable in the medium collected from the NSPs. Thus, while there are astrocyte progenitors and immature astrocytes within the neurospheres, our data suggest that these precursors are evidently not at a sufficient stage of maturation to render them competent to produce LIF. Supporting this view, the cells that expressed LIF mRNA most highly within the SVZ using smFISH tended to be adjacent to the medial SVZ rather than within it, consistent with the view that they were more mature. Notably, we did not observe any GFAP + cells with radially aligned GFAP mRNA dots, suggesting that the stem cells themselves are not producing LIF.

Altogether, these data indicate that Notch1 is an important contributor to the expansion of NSPs following perinatal H-I. These developmental brain injuries can be devastating to children and to those with the responsibility of caring for them. Current therapies do not provide sufficient improvement in neurologic function after such insults, and the burden they create demands that we seek new strategies. Neurogenesis offers important hope for repair and regeneration after brain injury. While increasing numbers of new neurons following perinatal H-I is an important step, future work is required to better understand how to stimulate the migration, maturation, and integration of these new cells. Understanding how increased Notch signaling in the context of perinatal H-I alters NSP proliferation will provide important clues as to how these valuable precursors can be mobilized to provide regenerative therapy.

ROLE OF AUTHORS

All authors had full access to all the data in the study and take responsibility for the integrity of the data and the accuracy of the data analysis. Study concept and design: RJF, MVC, MB, SWL. Acquisition of data: RJF, MVC, PW. Analysis and interpretation of data: RJF, MVC, MB, SWL. Drafting of the manuscript: RJF, SWL. Critical revision of the manuscript for important intellectual content: RJF, MVC, PW, MB. Statistical analysis: RJF, MVC. Obtained funding: RJF, SWL, MB. Study supervision: SWL.

REFERENCES

Ables JL, Breunig JJ, Eisch AJ, Rakic P. 2011. Not(ch) just development: Notch signalling in the adult brain. Nat Rev Neurosci 12:269–283.

Aguirre A, Rubio ME, Gallo V. 2010. Notch and EGFR pathway interaction regulates neural stem cell number and self-renewal. Nature 467: 323–327.

Alagappan D, Balan M, Jiang Y, Cohen RB, Kotenko SV, Levison SW. 2013. Egr-1 is a critical regulator of EGF-receptor-mediated expansion of subventricular zone neural stem cells and progenitors during recovery from hypoxia-hypoglycemia. ASN Neuro 5:183–193.

Androutsellis-Theotokis A, Leker RR, Soldner F, Hoeppner DJ, Ravin R, Poser SW, Rueger MA, Bae SK, Kittappa R, McKay RD. 2006. Notch signalling regulates stem cell numbers in vitro and in vivo. Nature 442:823–826.

Artavanis-Tsakonas S, Rand MD, Lake RJ. 1999. Notch signaling: cell fate control and signal integration in development. Science 284:770–776.

Arumugam TV, Chan SL, Jo DG, Yilmaz G, Tang SC, Cheng A, Gleichmann M, Okun E, Dixit VD, Chigurupati S, et al. 2006. Gamma secretase-mediated Notch signaling worsens brain damage and functional outcome in ischemic stroke. Nat Med 12:621–623.

Arumugam TV, Cheng YL, Choi Y, Choi YH, Yang S, Yun YK, Park JS, Yang DK, Thundyil J, Gelderblom M, et al. 2011. Evidence that gamma-secretase-mediated Notch signaling induces neuronal cell death via the nuclear factor-kappaB-Bcl-2-interacting mediator of cell death pathway in ischemic stroke. Mol Pharmacol 80:23–31.

Baik SH, Fane M, Park JH, Cheng YL, Yang-Wei Fann D, Yun UJ, Choi Y, Park JS, Chai BH, Park JS, et al. 2015. Pin1 promotes neuronal death in stroke by stabilizing Notch intracellular domain. Ann Neurol 77:504–516.

Basak O, Giachino C, Fiorini E, Macdonald HR, Taylor V. 2012. Neurogenic subventricular zone stem/progenitor cells are Notch1-dependent in their active but not quiescent state. J Neurosci 32:5654–5666.

Batish M, Raj A, Tyagi S. 2011. Single molecule imaging of RNA in situ. Methods Mol Biol 714:3–13.

Blaumueller CM, Qi H, Zagouras P, Artavanis-Tsakonas S. 1997. Intracellular cleavage of Notch leads to a heterodimeric receptor on the plasma membrane. Cell 90:281–291.

Buono KD, Goodus MT, Guardia Clausi M, Jiang Y, Loporchio D, Levison SW. 2015. Mechanisms of mouse neural precursor expansion after neonatal hypoxia-ischemia. J Neurosci 35:8855–8865.

Caille I, Allinquant B, Dupont E, Bouillot C, Langer A, Muller U, Prochiantz A. 2004. Soluble form of amyloid precursor protein regulates proliferation of progenitors in the adult subventricular zone. Development 131:2173–2181.

Carlen M, Meletis K, Goritz C, Darsalia V, Evergren E, Tanigaki K, Amendola M, Barnabe-Heider F, Yeung MS, Naldini L, et al. 2009. Forebrain ependymal cells are Notch-dependent and generate neuroblasts and astrocytes after stroke. Nat Neurosci 12:259–267.

Carroll CM, Li YM. 2016. Physiological and pathological roles of the gamma-secretase complex. Brain Res Bull doi: 10.1016/j.brainresbull.2016.04.019.

Chambers CB, Peng Y, Nguyen H, Gaiano N, Fishell G, Nye JS. 2001. Spatiotemporal selectivity of response to Notch1 signals in mammalian forebrain precursors. Development 128:689–702.

Chojnacki A, Shimazaki T, Gregg C, Weinmaster G, Weiss S. 2003. Glycoprotein 130 signaling regulates Notch1 expression and activation in the self-renewal of mammalian forebrain neural stem cells. J Neurosci 23:1730–1741.

Covey MV, Levison SW. 2007. Leukemia inhibitory factor participates in the expansion of neural stem/progenitors after perinatal hypoxia/ischemia. Neuroscience 148:501–509.

Cramer SC, Chopp M. 2000. Recovery recapitulates ontogeny. Trends Neurosci 23:265–271.

De Strooper B, Annaert W, Cupers P, Saftig P, Craessaerts K, Mumm JS, Schroeter EH, Schrijvers V, Wolfe MS, Ray WJ, et al. 1999. A presenilin-1-dependent gamma-secretase-like protease mediates release of Notch intracellular domain. Nature 398:518–522.

Dovey HF, John V, Anderson JP, Chen LZ, de Saint Andrieu P, Fang LY, Freedman SB, Folmer B, Goldbach E, Holsztynska EJ, et al. 2001. Functional gamma-secretase inhibitors reduce beta-amyloid peptide levels in brain. J Neurochem 76:173–181.

Ehm O, Goritz C, Covic M, Schaffner I, Schwarz TJ, Karaca E, Kempkes B, Kremmer E, Pfrieger FW, Espinosa L, et al. 2010. RBPJkappa-dependent signaling is essential for long-term maintenance of neural stem cells in the adult hippocampus. J Neurosci 30:13794–13807.

Felling RJ, Levison SW. 2003. Enhanced neurogenesis following stroke. J Neurosci Res 73:277–283.

Felling RJ, Snyder MJ, Romanko MJ, Rothstein RP, Ziegler AN, Yang Z, Givogri MI, Bongarzone ER, Levison SW. 2006. Neural stem/progenitor cells participate in the regenerative response to perinatal hypoxia/ischemia. J Neurosci 26:4359–4369.

Ferent J, Cochard L, Faure H, Taddei M, Hahn H, Ruat M, Traiffort E. 2014. Genetic activation of Hedgehog signaling unbalances the rate of neural stem cell renewal by increasing symmetric divisions. Stem Cell Reports 3:312–323.

Friedmann DR, Wilson JJ, Kovall RA. 2008. RAM-induced allostery facilitates assembly of a notch pathway active transcription complex. J Biol Chem 283:14781–14791.

Gaiano N, Fishell G. 2002. The role of notch in promoting glial and neural stem cell fates. Annu Rev Neurosci 25:471–490.

Gao F, Zhang Q, Zheng MH, Liu HL, Hu YY, Zhang P, Zhang ZP, Qin HY, Feng L, Wang L, et al. 2009. Transcription factor RBP-J-mediated signaling represses the differentiation of neural stem cells into intermediate neural progenitors. Mol Cell Neurosci 40:442–450.

Garcia-Verdugo JM, Doetsch F, Wichterle H, Lim DA, Alvarez-Buylla A. 1998. Architecture and cell types of the adult subventricular zone: in search of the stem cells. J Neurobiol 36:234–248.

Goings GE, Sahni V, Szele FG. 2004. Migration patterns of subventricular zone cells in adult mice change after cerebral cortex injury. Brain Res 996:213–226.

Guentchev M, McKay RD. 2006. Notch controls proliferation and differentiation of stem cells in a dose-dependent manner. Eur J Neurosci 23:2289–2296.

Gustafsson MV, Zheng X, Pereira T, Gradin K, Jin S, Lundkvist J, Ruas JL, Poellinger L, Lendahl U, Bondesson M. 2005. Hypoxia requires notch signaling to maintain the undifferentiated cell state. Dev Cell 9:617–628.

Hitoshi S, Alexson T, Tropepe V, Donoviel D, Elia AJ, Nye JS, Conlon RA, Mak TW, Bernstein A, van der Kooy D. 2002. Notch pathway molecules are essential for the maintenance, but not the generation, of mammalian neural stem cells. Genes Dev 16:846–858.

Imayoshi I, Sakamoto M, Yamaguchi M, Mori K, Kageyama R. 2010. Essential roles of Notch signaling in maintenance of neural stem cells in developing and adult brains. J Neurosci 30:3489–3498.

Ishibashi T, Dakin KA, Stevens B, Lee PR, Kozlov SV, Stewart CL, Fields RD. 2006. Astrocytes promote myelination in response to electrical impulses. Neuron 49:823–832.

Jang J, Byun SH, Han D, Lee J, Kim J, Lee N, Kim I, Park S, Ha S, Kwon M, et al. 2014. Notch intracellular domain deficiency in nuclear localization activity retains the ability to enhance neural stem cell character and block neurogenesis in mammalian brain development. Stem Cells Dev 23:2841–2850.

Kageyama R, Ohtsuka T, Hatakeyama J, Ohsawa R. 2005. Roles of bHLH genes in neural stem cell differentiation. Exp Cell Res 306:343–348.

Kopan R, Ilagan MX. 2009. The canonical Notch signaling pathway: unfolding the activation mechanism. Cell 137:216–233.

Markey FB, Ruezinsky W, Tyagi S, Batish M. 2014. Fusion FISH imaging: single-molecule detection of gene fusion transcripts in situ. PLoS One 9:e93488.

Marumo T, Takagi Y, Muraki K, Hashimoto N, Miyamoto S, Tanigaki K. 2013. Notch signaling regulates nucleocytoplasmic Olig2 translocation in reactive astrocytes differentiation after ischemic stroke. Neurosci Res 75:204–209.

Morshead CM, Reynolds BA, Craig CG, McBurney MW, Staines WA, Morassutti D, Weiss S, Van der Kooy D. 1994. Neural stem cells in the adult mammalian forebrain: a relatively quiescent subpopulation of subependymal cells. Neuron 13:1071–1082.

Mumm JS, Kopan R. 2000. Notch signaling: from the outside in. Dev Biol 228:151–165.

Ohtsuka T, Sakamoto M, Guillemot F, Kageyama R. 2001. Roles of the basic helix-loop-helix genes Hes1 and Hes5 in expansion of neural stem cells of the developing brain. J Biol Chem 276:30467–30474.

Pfaffl MW, Horgan GW, Dempfle L. 2002. Relative expression software tool (REST) for group-wise comparison and statistical analysis of relative expression results in real-time PCR. Nucleic Acids Res 30:e36.

Rice JE, Vannucci RC, Brierley JB. 1981. The influence of immaturity on hypoxic-ischemic brain damage in the rat. Ann Neurol 9:131–141.

Romanko MJ, Rola R, Fike JR, Szele FG, Dizon ML, Felling RJ, Brazel CY, Levison SW. 2004a. Roles of the mammalian subventricular zone in cell replacement after brain injury. Prog Neurobiol 74:77–99.

Romanko MJ, Rothstein RP, Levison SW. 2004b. Neural stem cells in the subventricular zone are resilient to hypoxia/ischemia whereas progenitors are vulnerable. J Cereb Blood Flow Metab 24:814–825.

Sanalkumar R, Dhanesh SB, James J. 2010. Non-canonical activation of Notch signaling/target genes in vertebrates. Cell Mol Life Sci 67:2957–2968.

Schroeter EH, Kisslinger JA, Kopan R. 1998. Notch-1 signalling requires ligand-induced proteolytic release of intracellular domain. Nature 393:382–386.

Shimada IS, LeComte MD, Granger JC, Quinlan NJ, Spees JL. 2012. Self-renewal and differentiation of reactive astrocyte-derived neural stem/progenitor cells isolated from the cortical peri-infarct area after stroke. J Neurosci 32:7926–7940.

Shimojo H, Ohtsuka T, Kageyama R. 2008. Oscillations in notch signaling regulate maintenance of neural progenitors. Neuron 58:52–64.

Sun F, Mao X, Xie L, Ding M, Shao B, Jin K. 2013. Notch1 signaling modulates neuronal progenitor activity in the subventricular zone in response to aging and focal ischemia. Aging Cell 12:978–987.

Szele FG, Chesselet MF. 1996. Cortical lesions induce an increase in cell number and PSA-NCAM expression in the subventricular zone of adult rats. J Comp Neurol 368:439–454.

Vannucci RC, Vannucci SJ. 2005. Perinatal hypoxic-ischemic brain damage: evolution of an animal model. Dev Neurosci 27: 81–86.

Wang J, Ye Z, Zheng S, Chen L, Wan Y, Deng Y, Yang R. 2016. Lingo-1 shRNA and Notch signaling inhibitor DAPT promote differentiation of neural stem/progenitor cells into neurons. Brain Res 1634:34–44.

Wu Y, Liu Y, Levine EM, Rao MS. 2003. Hes1 but not Hes5 regulates an astrocyte versus oligodendrocyte fate choice in glial restricted precursors. Dev Dyn 226:675–689.

Zhang K, Zhao T, Huang X, Wu LY, Wu K, Zhu LL, Fan M. 2014. Notch1 mediates postnatal neurogenesis in hippocampus enhanced by intermittent hypoxia. Neurobiol Dis 64:66–78.